

# IN-PLANE BEHAVIOUR OF MONO-SYMMETRIC TAPERED BEAMS

NICHOLAS TRAHAIR  
PETER ANSOURIAN

RESEARCH REPORT R957  
NOVEMBER 2015

ISSN 1833-2781

SCHOOL OF CIVIL  
ENGINEERING



THE UNIVERSITY OF  
SYDNEY



THE UNIVERSITY OF  
**SYDNEY**

SCHOOL OF CIVIL ENGINEERING

**IN-PLANE BEHAVIOUR OF MONO-SYMMETRIC TAPERED BEAMS**

**RESEARCH REPORT R957**

**NS TRAHAIR AND P ANSOURIAN**

NOVEMBER 2015

ISSN 1833-2781

**Copyright Notice**

School of Civil Engineering, Research Report R957  
NS Trahair and P Ansourian  
November 2015

ISSN 1833-2781

This publication may be redistributed freely in its entirety and in its original form without the consent of the copyright owner.

Use of material contained in this publication in any other published works must be appropriately referenced, and, if necessary, permission sought from the author.

Published by:  
School of Civil Engineering  
The University of Sydney  
Sydney NSW 2006  
Australia

This report and other Research Reports published by the School of Civil Engineering are available at  
<http://sydney.edu.au/civil>

## **ABSTRACT**

Shear stress distributions in mono-symmetric tapered I-beams are incorrectly predicted by the conventional beam analysis method used for uniform beams. More accurate predictions are obtained by assuming that the normal stress trajectories vary linearly between plate edges, instead of parallel to the centroidal axis.

Transverse shear stresses at the flange-web junctions of mono-symmetric tapered I-beams of constant depth are induced by gradients of the forces in the tapered flanges. The transverse shear stress distributions caused by axial force, moment, and shear force are constant, linear, and parabolic, respectively.

Axial force induces non-zero principal axis shear stresses, while shear force induces non-zero normal stresses acting parallel to the centroidal axis.

## **KEYWORDS**

Bending, deflections, elasticity, force, I-beam, mono-symmetry, normal stress, shear, shear stress, tapered flange, edge

## TABLE OF CONTENTS

ABSTRACT.....	3
KEYWORDS.....	3
TABLE OF CONTENTS.....	4
1 INTRODUCTION .....	5
2 THICKNESS TAPERED PLATES .....	5
2.1 Plates .....	5
2.2 Uniform Compression .....	5
2.3 Uniform Bending .....	5
3 MONO-SYMMETRIC TAPERED I-BEAMS.....	6
3.1 Beams .....	6
3.2 Methods of Analysis.....	6
3.3 Axial Compression.....	7
3.4 Moment .....	7
3.5 Shear.....	7
4 DISCUSSION AND CONCLUSIONS .....	7
5 REFERENCES .....	8
APPENDIX A THICKNESS TAPERED PLATES .....	8
APPENDIX B MONO-SYMMETRIC TAPERED I-BEAMS .....	10
B.1 Normal Stress Analysis .....	10
B.2 Shear Stress Analysis .....	10
NOTATION .....	12

## 1. INTRODUCTION

While the in-plane behaviour of doubly symmetric tapered I-beams has recently been analysed [1], mono-symmetric tapered beams (Fig. 1) are rarely if ever treated in textbooks. Designers commonly assume that tapered beams behave in the same way as uniform beams, and while this is satisfactory for the bending deflections and the normal stresses, it may lead to incorrect shear stress distributions.

In uniform mono-symmetric I-beams, the normal stresses due to moments and axial forces are parallel to the centroidal axis, while the shear forces are resisted solely by shear stresses in the web [2]. However, in mono-symmetric tapered I-beams, the flanges are inclined to the centroidal axis, as are the flange normal stresses, and so the stress trajectories are inclined to the centroidal axis. In addition, the inclined flange forces have components transverse to the centroidal axis, which participate in resisting the shear forces.

In this paper, the distributions of the normal and shear stresses in mono-symmetric tapered I-beams are investigated. First, the stress distributions in mono-symmetric thickness tapered plates (without flanges) (Fig. 2) are analysed, because of their similarity to tapered wedges (without flanges), whose known behaviour [3] suggested [1] that the normal stresses in web-tapered I-beams act along lines whose inclinations vary linearly between those of the plate edges. This suggestion is then used to analyse the distributions of normal and shear stresses in mono-symmetric tapered I-beams (Fig. 1). Finally, the predicted stress distributions are compared with those obtained from a more rigorous finite element computer program [4] which incorporates the two-dimensional membrane behaviour of the flange and web plates of which the tapered beams are composed.

## 2. TAPERED THICKNESS PLATES

### 2.1 Plates

A tapered rectangular plate  $d \times L \times t$  is shown in Fig. 2. The thickness  $t$  is tapered linearly along the length and down the depth. The thickness at the top LH and bottom RH corners is  $t_t$ , and at the bottom LH and top RH corners is  $t_b$ . The tapered thickness causes the plate to be mono-symmetric in cross-section and tapered along its length. The centroidal axis CC is inclined to the plate mid-line.

The conventional beam analysis (CBA) of uniform beams under axial compression and bending is adapted for tapered mono-symmetric plates in Appendix A by assuming that the normal stresses act along lines parallel to the longitudinal edges of the plates.

### 2.2 Uniform Compression

Uniform compression of the tapered plate induces uniform longitudinal normal stresses  $\sigma_z$  and transverse shear stresses  $\tau_{zy}$  which have a parabolic variation down the plate at mid-span from zero at the edges to a maximum at mid-depth, as shown in Fig. 3a.

These stresses may be converted to normal stresses  $\sigma_z$  parallel to the centroidal  $z$  axis and shear stresses  $\tau_{zy}$  parallel to the principal  $y$  axis by assuming that the normal stresses  $\sigma_y$  are zero, whence [3]

$$\begin{aligned}\sigma_z &= \sigma_z \cos^2 \theta + 2\tau_{zy} \sin \theta \cos \theta \\ \tau_{zy} &= \tau_{zy} (\cos^2 \theta - \sin^2 \theta) - \sigma_z \sin \theta \cos \theta\end{aligned}\tag{1}$$

in which  $\theta$  is the angle between the  $Z$  and the  $z$  axes. The principal axis stresses  $\sigma_z$  and  $\tau_{zy}$  are also shown in Fig. 3a. The resultant of the normal stresses  $\sigma_z$  is equal to the applied compression force, while the non-zero shear stresses  $\tau_{zy}$  have a zero stress resultant.

### 2.3 Uniform Bending

Uniform bending induces longitudinal normal stresses  $\sigma_z$  and shear stresses  $\tau_{zy}$ . At mid-span, the normal stresses vary linearly down the depth, and the self-equilibrating shear stresses have a cubic variation, as

shown in Fig. 3b. The corresponding principal axis stresses  $\sigma_z$  and  $\tau_{zy}$  are also shown in Fig. 3b. The resultant of the normal stresses  $\sigma_z$  is equal to the applied moment, while the non-zero shear stresses  $\tau_{zy}$  have a zero stress resultant.

### 3. MONO-SYMMETRIC TAPERED I-BEAMS

#### 3.1 Beams

A mono-symmetric I-beam of constant depth and reversed tapered flanges is shown in Fig. 1. Its centroidal axis CC is inclined. The beam length is  $L = 152$  mm. The cross-section dimensions are shown in Table 1.

Table 1. Cross-Section Dimensions

Dimension	Section 1	Section 2
$Z$ (mm)	-76	76
$b_f$ (mm)	17.67	31.55
$b_b$ (mm)	31.55	17.67
$b_w$ (mm)	72.76	72.76
$t_f$ (mm)	3.11	3.11
$t_w$ (mm)	2.13	2.13

#### 3.2 Methods of Analysis

##### 3.2.1 Tapered Beam Analysis (TBA)

The methods of linear elastic analysis (CBA) of uniform beams are well documented [2]. In summary, plane sections are assumed to remain plane, shear strains are neglected in the analysis of the bending deflections, and stress concentrations at applied loads or reactions are ignored. The section properties of area  $A$  and second moment of area  $I_x$  are used to determine the longitudinal normal stresses  $\sigma$  caused by axial force  $N$  and bending moment  $M$ , which are determined from the applied loads and moments either by equilibrium for determinate beams or by analysis of the bending deflections  $v$  for indeterminate beams. In Appendix B, CBA analysis of bending and compression is adapted for mono-symmetric tapered I-beams by assuming that the normal stress trajectory inclinations vary linearly between those of the edges of the plates of which the beam is composed. This adapted analysis using inclined stress trajectories is referred to in this paper as tapered beam analysis (TBA).

##### 3.2.2 Finite Element Analysis (FEA)

For this paper, the bending and compression of tapered I-beams has been analysed (FEA) by using the finite element computer program STRAND7 [4]. This software contains a variety of plate/shell elements for the analysis of plane stress/strain/axisymmetric and general shell structures. In the context of this paper, the QUAD4 plate/shell element has been used for the analysis of tapered flange problems. The element provides high accuracy for relatively coarse meshes and is well suited for the analysis of I-section beams modelled with 3 plates for the two flanges and the web, any of which can be tapered in their own plane. The element is based on conventional thin plate theory, and can tolerate skews in the range 45-135 degrees, and aspect ratios up to 4. In regions of high stress gradient, the skew should be closer to 90 degrees and the aspect ratio closer to one. The state of stress within a flange or web is one of plane stress including membrane normal and shear stresses. Local stress concentrations are captured in the neighbourhood of applied nodal forces.

### 3.3 Axial Compression

The constant depth mono-symmetric I-beam with reverse tapered flanges shown in Fig. 4a has two collinear equal and opposite inclined compression forces  $-N$  acting at the end centroids. The mid-span stresses within this beam have been analysed (TBA) in Appendix B using web stress trajectories parallel to the flanges. The normal stresses  $\sigma_z$  are constant across the section, as are the web shear stresses  $\tau_{zy}$ , as shown diagrammatically in Fig. 4a. The resultants of these stresses are equal to the horizontal and vertical components of the inclined compression  $-N$ .

The principal axis stresses  $\sigma_z$  and  $\tau_{zy}$  are also shown diagrammatically in Fig. 4a. The non-zero resultant of the shear stresses  $\tau_{zy}$  balances the  $y$  direction components of the flange forces, so that there is no net force in the  $y$  direction. These stresses are not predicted by CBA.

The stresses within this beam have also been determined by FEA [4]. The length of this beam is very short, so that significant shear effects and end stress concentrations may occur. The values of the mid-span stresses at the top flange-web junction and mid web depth are close to those determined by TBA, as shown in Table 2. The small discrepancies may be due to the assumption made in Appendix B that  $\theta$  is small, and due to the effects of stress concentrations on the FEA results.

Table 2 Comparison of Mid-Span Stresses

Figure	Loading	Analysis	$\sigma_{zi}$ (N/mm <sup>2</sup> )	$\sigma_{sz0}$ (N/mm <sup>2</sup> )	$\tau_{zyi}$ (N/mm <sup>2</sup> )	$\tau_{zy0}$ (N/mm <sup>2</sup> )
4a	$N = -1E4$ N	TBA	-32.5	-32.5	4.3	4.3
		FEA	-32.4	-32.4	4.3	4.3
4b	$M = 1E5$ Nmm	TBA	-15.1	0	1.0	0
		FEA	-15.0	0	0.9	0
4c	$M = 76E4$ Nmm $V = 1E4$ N	TBA	0	0	48.2	72.7
		FEA	1.3	-4.0	50	72.3

### 3.4 Moment

The mono-symmetric tapered beam shown in Fig. 4b has two equal and opposite end moments  $M$ . The mid-span stresses within this beam have been determined by TBA. The horizontal normal stresses  $\sigma_z$  vary linearly across the section, as do the self-equilibrating web vertical shear stresses  $\tau_{zy}$ , as shown diagrammatically in Fig. 4b. These stresses are equivalent to a linearly varying set of normal stresses  $\sigma_z$  parallel to the centroidal  $z$  axis, and a zero set of shear stresses  $\tau_{zy}$  parallel to the  $y$  principal axis.

The stresses within this beam have also been determined by FEA. The values of the mid-span stresses are close to those determined by TBA, as shown in Table 2.

### 3.5 Shear

The mono-symmetric tapered beam shown in Fig. 4c has two equal and opposite end shears  $V$  and equal end reaction moments  $M = VL/2$ . The mid-span stresses within this beam have been determined by TBA. The horizontal normal stresses  $\sigma_z$  are zero while the shear stresses  $\tau_{zy}$  vary parabolically across the section, as shown diagrammatically in Fig. 4c. The corresponding normal stresses  $\sigma_z$  parallel to the centroidal  $z$  axis and shear stresses  $\tau_{zy}$  parallel to the  $y$  principal axis are also shown in Fig. 4c.

The stresses within this beam have also been determined by FEA. The values of the mid-span stresses are close to those determined by TBA, as shown in Table 2.

## 4. DISCUSSION AND CONCLUSIONS

Free edges or junctions of plate components enforce parallel adjacent normal stress trajectories, even when these are inclined to the centroidal axis. The assumption of inclined stress trajectories in the analysis of doubly symmetric web-tapered I-beams has led to stress predictions [1] which are in close agreement with

more accurate finite element results. In this paper, this assumption has been used to analyse (TBA) the stress distributions in thickness tapered plates and mono-symmetric tapered I-beams of constant depth, whose centroidal axes are inclined to the plate edges. This has led to normal stress and deflection magnitudes which are the same as those predicted by conventional beam analysis (CBA) based on the assumption that the normal stress trajectories are parallel to the centroidal axis. However, the shear stress distributions predicted by CBA are markedly different from those of TBA.

Non-zero distributions of the principal axis shear stresses  $\tau_{yz}$  (but with zero stress resultants) are predicted for thickness tapered plates under uniform compression or bending, instead of the zero distributions of CBA.

In mono-symmetric tapered I-beams of constant depth under uniform compression, CBA also predicts a zero principal axis shear stress distribution, but there are shear stresses which have a non-zero stress resultant which counters the flange force components perpendicular to the centroidal axis. On the other hand, there is a zero principal shear stress distribution caused by uniform bending, as predicted by CBA.

The transverse shear stresses  $\tau_{yz}$  determined by TBA are in good agreement with the more accurate stresses determined by finite element analysis (FEA).

## 5. REFERENCES

- [1] Trahair, NS, and Ansourian, P, "In-Plane Behaviour of Web-Tapered Beams", *Research Report R956*, School of Civil Engineering, The University of Sydney, October, 2015.
- [2] Trahair, NS, Bradford, MA, Nethercot, DA, and Gardner, L, *The Behaviour and Design of Steel Structures to EC3*, 4<sup>th</sup> ed., Taylor and Francis, London, 2008.
- [3] Timoshenko, SP, and Goodier, JN, *Theory of Elasticity*, 2<sup>nd</sup> ed., McGraw-Hill, New York, 1951.
- [4] Strand7 Pty Ltd, *STRAND7*, Sydney, 2015.

## APPENDIX A. THICKNESS TAPERED PLATES

A tapered rectangular plate  $d \times L \times t$  is shown in Fig. 2. The longitudinal Z axis is along the plate midline and the Y axis is down the web. The thickness is tapered linearly along the length and down the depth. The thickness at the top LH and bottom RH corners is  $t_t$  and at the bottom LH and top RH corners is  $t_b$ . The variation of the thickness throughout the plate is given by

$$t = t_0 + Yt_1 \quad (\text{A.1})$$

in which

$$\begin{aligned} t_0 &= (t_b + t_t)/2 \\ t_1 &= -(2/d)(2Z/L)(t_b - t_t)/2 \end{aligned} \quad (\text{A.2})$$

The section properties may be defined by

$$\begin{aligned} A &= \int_{-d/2}^{d/2} t dY = dt_0 \\ Y_c &= \int_{-d/2}^{d/2} Y t dY / A = d^2 t_1 / 12t_0 \\ I_x &= \int_{-d/2}^{d/2} (Y - Y_c)^2 t dY = (d^3 t_0 / 12)(1 - d^2 t_1^2 / 12t_0^2) \end{aligned} \quad (\text{A.3})$$

The plate has equal and opposite end moments  $M$  and equal and opposite end forces  $N$  acting along the centroidal axis. These cause the plate to deflect  $w$  along the Z axis and  $v$  down the Y axis. The displacement of a point P(Z, Y) is given by

$$w_P = w - Yv' \quad (\text{A.4})$$

so that the horizontal normal strains and stresses (along the line  $Y = \text{constant}$ ) are

$$\begin{aligned} \varepsilon_Z &= w' - Yv'' \\ \sigma_Z &= E\varepsilon \end{aligned} \quad (\text{A.5})$$

in which  $' \equiv d/dZ$ .

The stress resultants are

$$\begin{aligned} N &= \int_{-d/2}^{d/2} \sigma_Z t dY = EA(w' - Y_c v'') \\ M &= \int_{-d/2}^{d/2} \sigma_Z (Y - Y_c) t dY = -EI_x v'' \end{aligned} \quad (\text{A.6})$$

The horizontal normal stresses can be expressed as

$$\sigma_Z = N/A + M(Y - Y_c)/I_x \quad (\text{A.7})$$

Equations A.6 and A.7 are the same as those used in the elastic analysis of uniform beams under bending and compression. They are independent of the taper.

These normal stresses induce vertical shear stresses  $\tau_{ZY}$  which can be determined from the equilibrium equation

$$d(\sigma_Z t)/dZ + d(\tau_{ZY} t)/dY = 0 \quad (\text{A.8})$$

whence

$$\tau_{ZY} t = (\tau_{ZY} t)_n + (\tau_{ZY} t)_m \quad (\text{A.9})$$

in which

$$\begin{aligned} (\tau_{ZY} t)_n &= \frac{N}{2L} \left( \frac{t_b - t_t}{t_b + t_t} \right) \left\{ \left( \frac{2Y}{d} \right)^2 - 1 \right\} \\ (\tau_{ZY} t)_m &= \frac{2M}{Ld} \left( \frac{t_b - t_t}{t_b + t_t} \right) \frac{(1 + d^2 t_1^2 / 12t_0^2)}{(1 - d^2 t_1^2 / 12t_0^2)^2} \left\{ \left( \frac{2Y}{d} \right)^3 - \frac{2Y}{d} \right\} \end{aligned} \quad (\text{A.10})$$

The stress resultant of the shear flow  $(\tau_{ZY} t)_n$  is the shear force

$$V = \int_{-d/2}^{d/2} (\tau_{ZY} t)_n dY = -\frac{N}{3L} \left( \frac{t_b - t_t}{t_b + t_t} \right) = NY_c' \quad (\text{A.11})$$

which is the vertical component of the inclined force  $N$ . The stress resultant of the shear flow  $(\tau_{ZY} t)_m$  is zero.

## APPENDIX B. MONO-SYMMETRIC TAPERED I-BEAMS

### B.1 Normal Stress Analysis

The mono-symmetric cross-sections shown in Fig. 1a and Fig. 1c have top and bottom flange and web widths  $b_t$ ,  $b_b$ , and  $b_w$  and thicknesses  $t_f$ ,  $t_f$ , and  $t_w$ , respectively. The tapered element shown in Fig. 1b has linearly tapered flange widths, but the web depth is constant. The element has an arbitrary but convenient [7] longitudinal axis OZ which is the locus of the web mid-heights, and a perpendicular axis OY which coincides with the web mid-thickness line, as shown in Fig. 1b.

The analysis of the normal strains and stresses caused by the bending and compression of a the tapered I-beam is similar to that given in Appendix A for thickness tapered plates, except for the section properties.

The section area of the tapered I-beam is

$$A = (b_t + b_b)t_f + b_w t_w \quad (\text{B.1})$$

The position of the centroid C is defined by the distance from the OZ axis

$$Y_c = \frac{b_w}{2} \frac{(b_b - b_t)t_f}{A} \quad (\text{B.2})$$

The major axis second moment of area is

$$\begin{aligned} I_x &= \int_A (Y - Y_c)^2 dA \\ &= b_b t_f (b_w / 2 - Y_c)^2 + b_t t_f (b_w / 2 + Y_c)^2 + b_w t_w Y_c^2 + b_w^3 t_w / 12 \end{aligned} \quad (\text{B.3})$$

### B.2 Shear Stress Analysis

Shear stresses  $\tau_{YZt}$  at the top flange-web junction of the beam in Fig. 1 are induced to balance the variations of the normal flange force  $N_{ft} = \sigma_{Zt} b_t t_f$ , whence

$$\tau_{YZt} t_w = -\frac{dN_{ft}}{dZ} = -\frac{d(\sigma_{Zt} b_t t_f)}{dZ} \quad (\text{B.4})$$

in which the top flange stress  $\sigma_{Zt}$  is obtained from Equation A.7 as

$$\sigma_{Zt} = N / A + My_t / I_x \quad (\text{B.5})$$

in which  $y_t = -(b_w / 2 + Y_c)$ . Thus

$$\frac{dN_{ft}}{dZ} = \frac{Nb_t t_f}{A} \left\{ \frac{1}{b_t} \frac{db_t}{dZ} - \frac{1}{A} \frac{dA}{dZ} \right\} = \frac{2Nt_f \alpha_t}{A} \quad (\text{B.6})$$

in which  $\alpha_t$  is the taper half angle of the top flange, and

$$\frac{dN_{ft}}{dZ} = \frac{Mb_t t_f y_t}{I_x} \left\{ \frac{1}{M} \frac{dM}{dZ} + \frac{1}{y_t} \frac{dy_t}{dZ} + \frac{1}{b_t} \frac{db_t}{dZ} - \frac{1}{I_x} \frac{dI_x}{dZ} \right\} \quad (\text{B.7})$$

in which

$$\frac{dI_x}{dZ} = -\frac{8\alpha_t^2 t_f^2 b_w^2 Z}{A} \quad (\text{B.8})$$

and

$$\frac{dy_t}{dZ} = -\theta = -\frac{dY_c}{dZ} = \frac{2\alpha_t t_f b_w}{A} \quad (\text{B.9})$$

At  $Z = 0$ ,  $Y_c = 0$ ,  $b_t = b_0$ ,  $y_t = -b_w/2$ ,  $dI_x/dZ = 0$ , so that

$$\tau_{YZt} t_w = -\frac{2Nt_f \alpha_t}{A} + \frac{Mb_0 t_f b_w}{2I_x} \left\{ \frac{V}{M} - \frac{4\alpha_t t_f}{A} + \frac{2\alpha_t}{b_0} \right\} \quad (\text{B.10})$$

In the web,

$$\frac{d\tau_{ZY}}{dY} = -\frac{d\sigma_Z}{dZ} \quad (\text{B.11})$$

or

$$\frac{d\tau_{YZ}}{dY} = -\frac{My}{I_x} \left( \frac{1}{M} \frac{dM}{dZ} + \frac{1}{y} \frac{dy}{dZ} - \frac{1}{I_x} \frac{dI_x}{dZ} \right) \quad (\text{B.12})$$

Thus at  $Z = 0$ ,

$$\tau_{YZ} = -\frac{VY^2}{2I_x} - \frac{MY}{I_x} \frac{2\alpha_t t_f b_w}{A} + \tau_0 \quad (\text{B.13})$$

The constant of integration  $\tau_0$  can be determined by equating the expression for  $\tau_{YZ}$  obtained from Equation B.13 by setting  $Y = -b_w/2$  to that obtained from Equation B.10. This allows Equation B.13 to be expressed as

$$\tau_{YZ} = \tau_{nt} + \tau_{mt} 2Y/b_w + \tau_{vt} + (\tau_{v0} - \tau_{vt})(1 - 8Y^2/b_w^2) \quad (\text{B.14})$$

in which

$$\begin{aligned} \tau_{nt} &= -\frac{2Nt_f \alpha_t}{At_w} \\ \tau_{mt} &= \frac{M \alpha_t t_f b_w^2}{I_x A} \\ \tau_{vt} &= \frac{Vb_w b_0 t_f}{2I_x} \\ \tau_{v0} &= \frac{Vb_w^2}{8I_x} \left\{ 1 + \frac{4b_0 t_f}{b_w t_w} \right\} \end{aligned} \quad (\text{B.15})$$

## NOTATION

$A$	Area of cross section
$b_{b,t}$	Widths of bottom and top flanges
$b_w$	Web depth
$d$	Plate depth
$E$	Young's modulus of elasticity
$I_x$	In-plane second moment of area
$L$	Length
$M$	Moment
$N$	Axial force
$N_f$	Flange force
$t_{b,t}$	Bottom and top flange thicknesses
$t_{f,w}$	Flange and web thicknesses
$v, w$	Displacements in $Y, Z$ directions
$V$	Shear force
$v_P, w_P$	Displacements of $P(Z, Y)$
$x, y$	Principal axes
$Y, Z$	Vertical and horizontal axes
$Y_c$	Distance to centroid
$z$	Distance along centroidal axis
$\alpha_t$	Taper angle of the top flange
$\varepsilon_z$	Strain
$\theta$	Angle between $Z$ and $z$ axes
$\sigma_z, \sigma_z$	Normal stresses in $Z, z$ directions
$\tau_{ZY}, \tau_{zy}$	Shear stresses in $Y, y$ directions

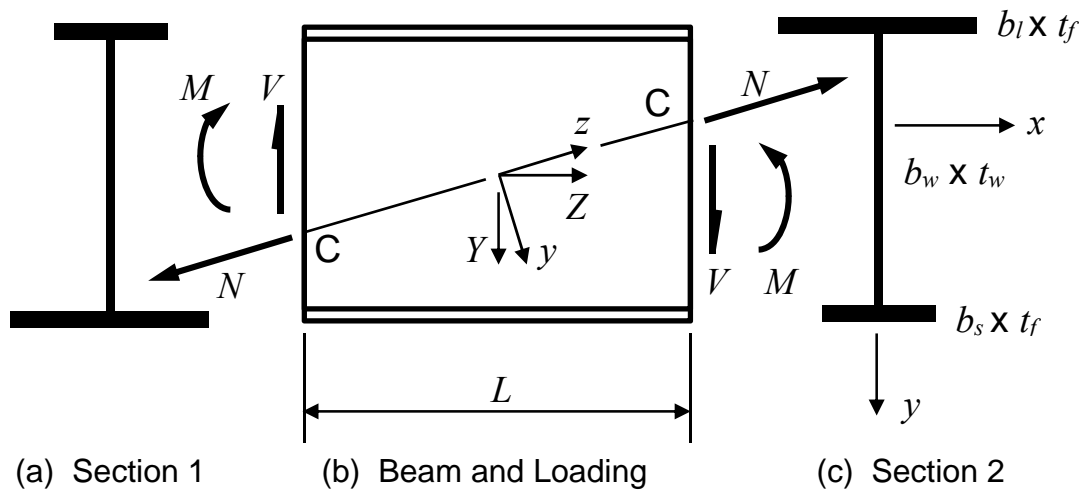


Fig. 1 Mono-Symmetric Tapered I-Beam

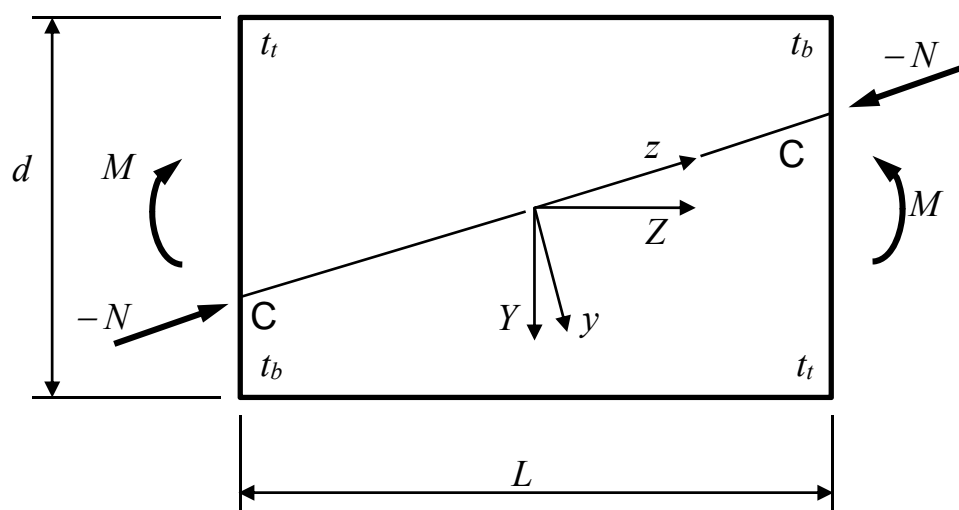


Fig. 2 Tapered Mono-Symmetric Plate

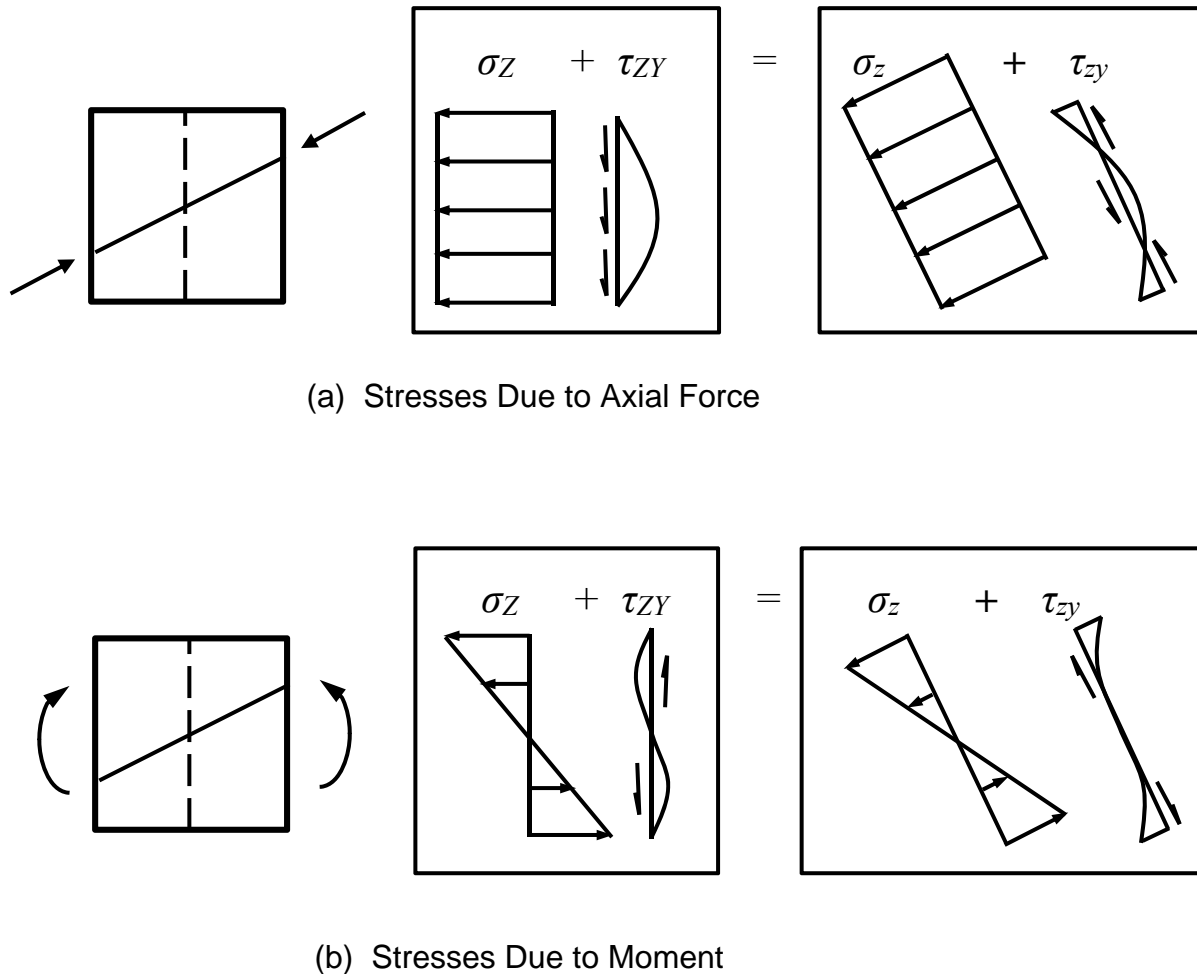
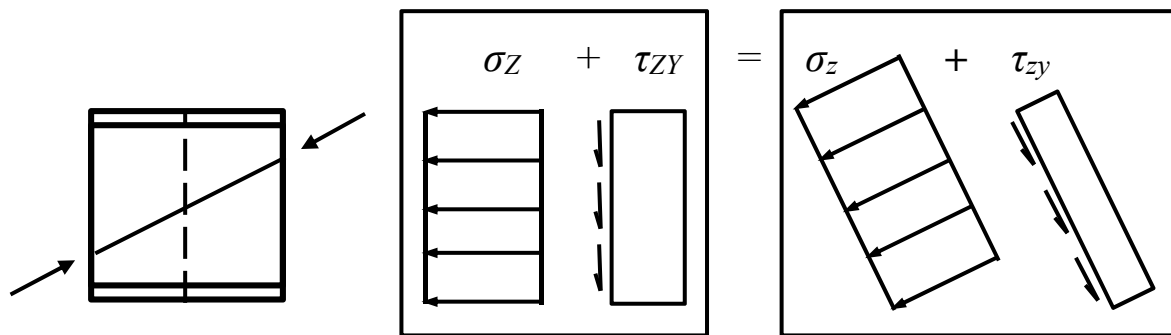
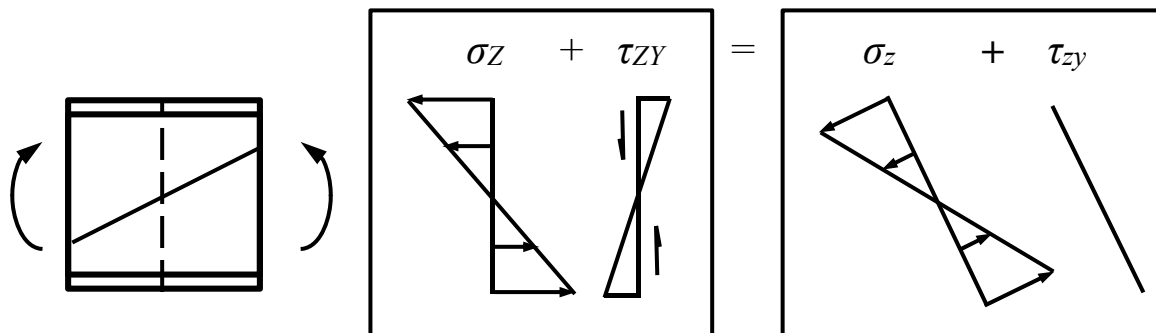


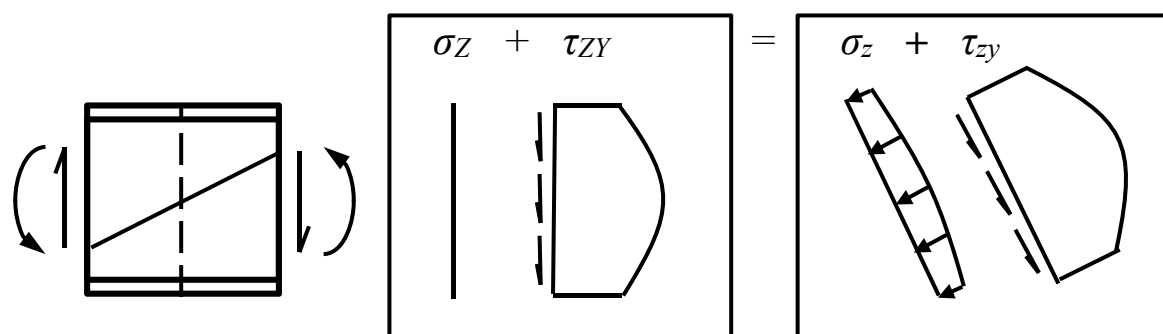
Fig. 3 Mid-Span Stresses in Tapered Plates



(a) Stresses Due to Axial Force



(b) Stresses Due to Moment



(c) Stresses Due to Shear

Fig. 4 Mid-Span Stresses in Tapered I-Beams